



# Structure and properties of barium ferrite powders prepared by milling and annealing

R. Nowosielski <sup>a</sup>, R. Babilas <sup>a,\*</sup>, G. Dercz <sup>b</sup>, L. Pająk <sup>b</sup>, J. Wrona <sup>c</sup>

<sup>a</sup> Division of Nanocrystalline and Functional Materials and Sustainable Pro-ecological Technologies, Institute of Engineering Materials and Biomaterials, Silesian University of Technology, ul. Konarskiego 18a, 44-100 Gliwice, Poland

<sup>b</sup> Institute of Materials Science, University of Silesia, ul. Bankowa 12, 40-007 Katowice, Poland

<sup>c</sup> Department of Electronics, AGH University of Science and Technology, Al. Mickiewicza 30, 30-059 Kraków, Poland

\* Corresponding author: E-mail address: rafal.babilas@polsl.pl

Received 23.10.2007; published in revised form 01.12.2007

## ABSTRACT

**Purpose:** Microstructure and magnetic properties analysis of barium ferrite powder obtained by milling and heat treatment

**Design/methodology/approach:** The milling process was carried out in a vibratory mill, which generated vibrations of the balls and milled material inside the container. After milling process the powders were annealed in electric chamber furnace. The X-ray diffraction methods were used for qualitative phase analysis of studied powder samples. The morphology of  $\text{Fe}_2\text{O}_3$  and  $\text{BaCO}_3$  powders after milling was analyzed using the scanning electron microscopy (SEM) method. The distribution of powder particles was determined by a laser particle analyzer. The magnetic hysteresis loops of examined powder material were measured by resonance vibrating sample magnetometer (R-VSM).

**Findings:** The milling process of iron oxide and barium carbonate mixture causes decrease of the crystallite size of involved phases and leads to increase the content of  $\text{Fe}_2\text{O}_3$  phase and decrease of  $\text{BaCO}_3$  content. Milling process causes enriching of surface layer of powder particles by  $\text{Fe}_2\text{O}_3$ . The X-ray investigations of tested mixture milled for 30 hours and annealed at  $950^\circ\text{C}$  enabled the identification of hard magnetic  $\text{BaFe}_{12}\text{O}_{19}$  phase and also the presence of  $\text{Fe}_2\text{O}_3$  phase in examined material. The  $\text{Fe}_2\text{O}_3$  phase is a rest of  $\text{BaCO}_3$  dissociation in the presence of  $\text{Fe}_2\text{O}_3$ , which forms a compound of  $\text{BaFe}_{12}\text{O}_{19}$ . The best coercive force for the mixture of powders annealed at  $950^\circ\text{C}$  for 10, 20 and 30 hours is 349 kA/m, 366 kA/m and 364 kA/m, respectively. From morphology images and distribution of powder particle size it can be concluded, that the size of tested powder particles increases with increasing time of milling process. The increase of milling time up to 20 hours leads to joining of smaller particles in bigger ones; agglomerates are formed.

**Practical implications:** The barium ferrite powder obtained by milling and annealing can be suitable component to produce sintered and elastic magnets with polymer matrix.

**Originality/value:** The results of tested barium ferrite investigations by different methods confirm their utility in the microstructure and magnetic properties analysis of powder materials.

**Keywords:** X-ray phase analysis; R-VSM; High-energy ball milling; Barium ferrite

## METHODOLOGY OF RESEARCH, ANALYSIS AND MODELLING

## 1. Introduction

Barium ferrites are well known hard magnetic materials, which are based on iron oxide. They are also called as ferrite magnets and could not be easily replaced by any other magnets [1-4].

Hexagonal barium ferrite having the chemical formula of  $\text{BaFe}_{12}\text{O}_{19}$  are widely used in magnetic recording media, microwave devices and electromagnetic shielding fields [5,6]. Barium ferrite possesses relatively high Curie temperature, coercive force and magnetic anisotropy field, as well as its excellent chemical stability and corrosion resistivity [7,8].

Ferrite magnets are still widely used although they have less magnetic strength than rare earth magnets. Comparing ferrite magnets and rare earth magnets could be concluded by determining the ratio of remanence ( $B_r$ ), which is about 1:3, the ratio of coercive force ( $H_c$ ), which is also 1:3 and the ratio of the maximum energy product  $(\text{BH})_{\text{max}}$ , which is about 1:10.

Many methods of synthesis have been developed to obtain a low production cost of powder particles of barium ferrite. The rare earth magnets are used where weight and size are very important from the cost and performance point of view [9,10].

The chemical compositions of the typical hard magnetic ferrite compounds are presented in Table 1. Magnetic properties of commercial ferrite magnets are shown in Figure 1. Figure 2 shows a phase diagram of  $\text{Fe}_2\text{O}_3$  – BaO system. The barium ferrite

phase with chemical composition of  $\text{BaO}6\text{Fe}_2\text{O}_3$  is visible in the region of system, where a content of BaO is about 15 mol.% [10].

The aim of this paper is the microstructure analysis and magnetic properties characterization of  $\text{BaFe}_{12}\text{O}_{19}$  powder obtained by milling and heat treatment.

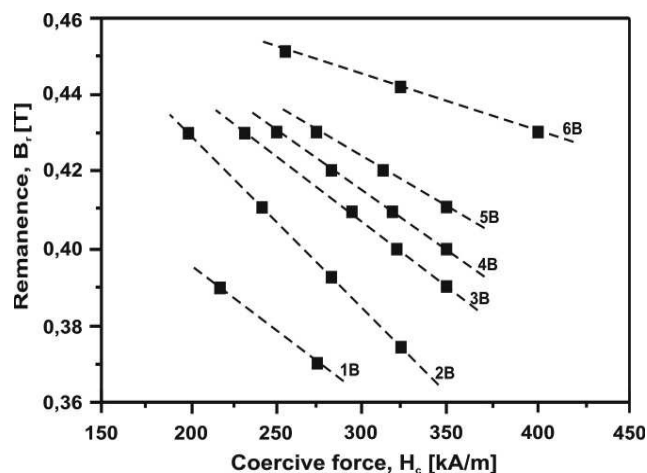


Fig. 1. Magnetic properties of Hitachi Metals ferrite magnets series YBM (1B–6B) [10]

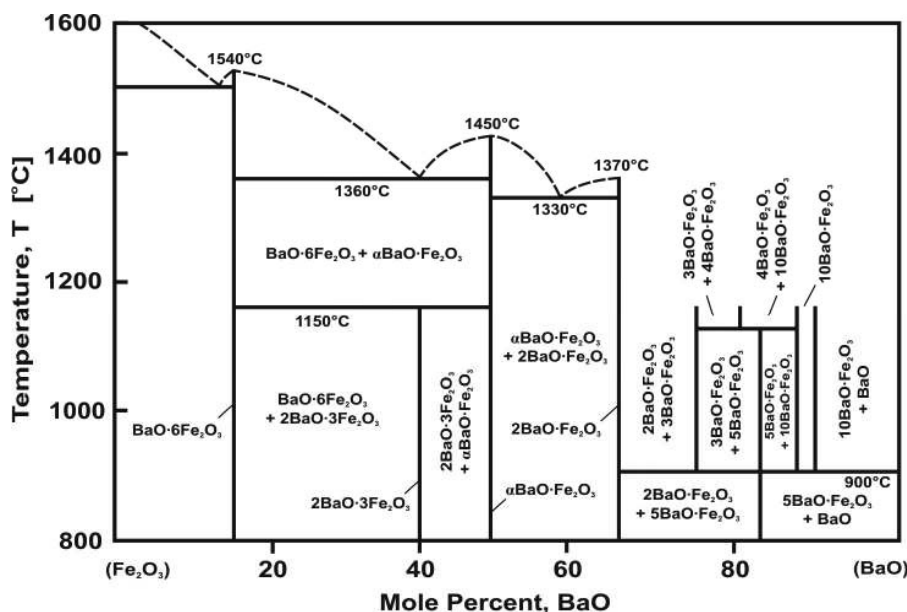


Fig. 2. Phase diagram of  $\text{Fe}_2\text{O}_3$  - BaO system [10]

Table 1.

Chemical composition of  $\text{BaO-MeO-Fe}_2\text{O}_3$  hexagonal magnetic compounds (MeO – metal oxide) [10]

No.	Molecular formula	Chemical composition (mol.%)		
		MeO	BaO	$\text{Fe}_2\text{O}_3$
1.	$\text{BaO} \cdot 6\text{Fe}_2\text{O}_3$	-	14.29	85.71
2.	$2\text{MeO} \cdot \text{BaO} \cdot 8\text{Fe}_2\text{O}_3$	18.18	9.09	72.71
3.	$2\text{MeO} \cdot 2\text{BaO} \cdot 6\text{Fe}_2\text{O}_3$	20	20	60
4.	$2\text{MeO} \cdot 3\text{BaO} \cdot 12\text{Fe}_2\text{O}_3$	11.76	17.65	70.59

## 2. Material and research methodology

For synthesis of  $\text{BaFe}_{12}\text{O}_{19}$ , mixture of iron oxide  $\text{Fe}_2\text{O}_3$  (99% purity) and barium carbonate  $\text{BaCO}_3$  (99% purity) powders was used with composition  $1.1\text{BaCO}_3 + 6\text{Fe}_2\text{O}_3$  (Fig.3.).

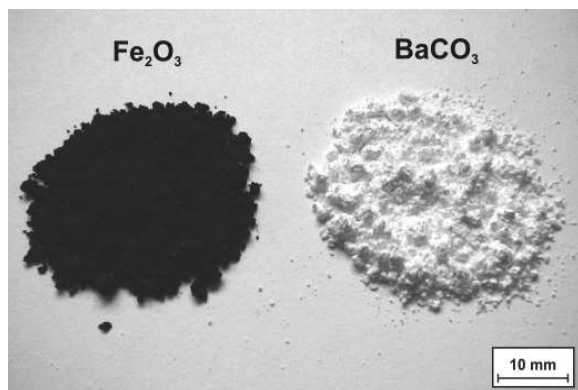


Fig. 3. External morphology of  $\text{Fe}_2\text{O}_3$  and  $\text{BaCO}_3$  powders used for milling process

Ball milling process was carried out in a vibratory mill type SPEX 8000 CertiPrep Mixer/Mill for 10, 20 and 30 hours under argon atmosphere. The weight ratio of balls to milled material was 5:1. The mill generated vibrations of the balls and the material inside the container [11,12].

After milling process the powders were annealed in the electric chamber furnace THERMOLYNE 6020C in 900, 950 and 1000°C in the air at atmosphere pressure for 1 hour.

Phase analysis was carried out using the X-Pert Philips diffractometer equipped with curved graphite monochromator on diffracted beam and a tube provided with copper anode. It was supplied by current intensity of 30 mA and voltage of 40 kV.

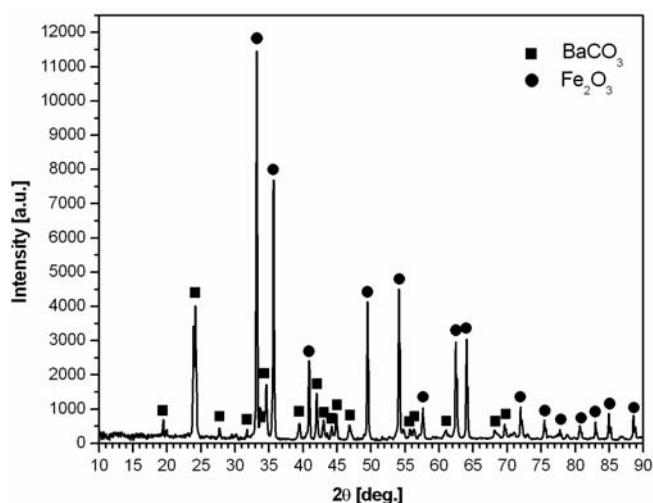


Fig. 4. X-ray diffraction pattern of  $\text{Fe}_2\text{O}_3$  and  $\text{BaCO}_3$  mixture as a starting material for milling

The length of radiation ( $\lambda_{\text{CuK}\alpha}$ ) was 1.54178 Å. The data of diffraction lines were recorded by “step-scanning” method in  $2\theta$  range from  $10^\circ$  to  $90^\circ$  and  $0.05^\circ$  step.

The Rietveld analysis was performed applying DBWS-9807 program that is an update version for Rietveld refinement with PC and mainframe computers [13]. The pseudo-Voigt function was used in the describing of diffraction line profiles at Rietveld refinement. The phase abundance was determined using the relation proposed by Hill and Howard [14-16].

The magnetic hysteresis loops of obtained powder material were measured by the Resonance Vibrating Sample Magnetometer (R-VSM). The idea of R-VSM is based on the Faraday induction law and the original Foner solution [17]. As distinct from Foner's VSM in the R-VSM sample oscillations are forced by piezoelectric transducer. Sample oscillates parallelly to the direction of external magnetic field and configuration of pick-up coils in the form of small Smith coils were applied.

The morphology of  $\text{Fe}_2\text{O}_3$  and  $\text{BaCO}_3$  powders after milling was analyzed using the OPTON DS940 scanning electron microscope with the ISIS software for the computer recording of images.

The diameter sizes of examined powder particles were determined using Fritsch Particle Sizer “Analysette 22” in measuring range from 0,1  $\mu\text{m}$  to 1180  $\mu\text{m}$ .

## 3. Results and discussion

Comparison of diffraction patterns of  $\text{Fe}_2\text{O}_3$  and  $\text{BaCO}_3$  mixture before milling (Fig.4) and after 30 hours of milling (Fig.5) shows the broadening of diffraction lines and decrease of their intensity. These effects indicate that ball milling causes decrease of the crystallite size of tested phases and leads to homogenizing the milled mixture. Statement the diffraction patterns of as-prepared and milled powders at different times are shown in Figure 6.

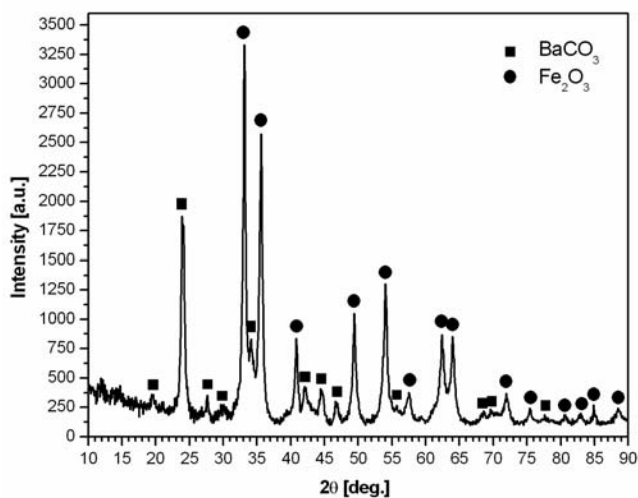


Fig. 5. X-ray diffraction pattern of  $\text{Fe}_2\text{O}_3$  and  $\text{BaCO}_3$  mixture after 30 hours of milling

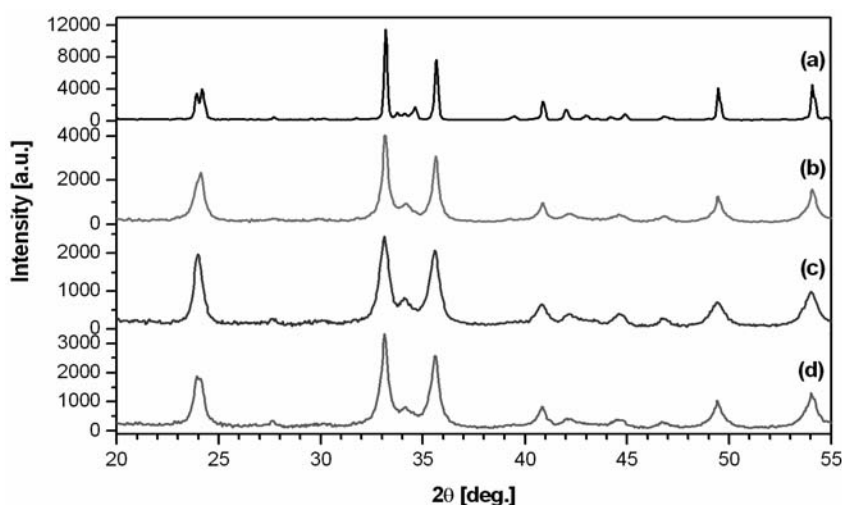


Fig. 6. X-ray diffraction patterns of  $\text{Fe}_2\text{O}_3$  and  $\text{BaCO}_3$  mixture after different times of milling: a) as-prepared, b) 10 h, c) 20 h, d) 30 h

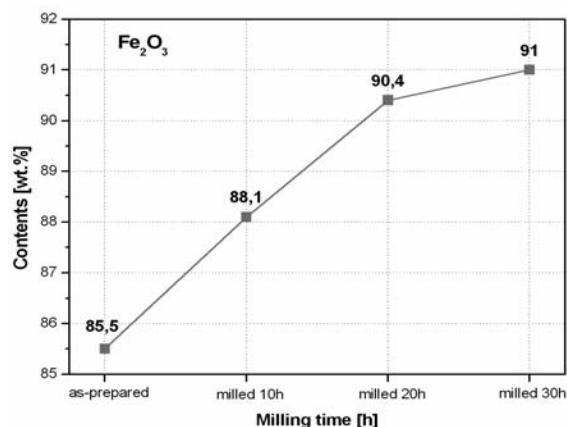


Fig. 7. Contents of  $\text{Fe}_2\text{O}_3$  phase in as-prepared state and after different times of milling

The iron oxide ( $\text{Fe}_2\text{O}_3$ ) phase appeared to be the main component of the tested mixture in as-prepared state (85.5 wt.%). On the other hand the content of  $\text{BaCO}_3$  phase is much lower (14.5 wt.%).

The milling process of examined  $\text{Fe}_2\text{O}_3$  and  $\text{BaCO}_3$  mixture leads to increase the content of  $\text{Fe}_2\text{O}_3$  phase and decrease the content of  $\text{BaCO}_3$  (Fig.7,8). After 30 hours of high-energy ball milling the content of  $\text{Fe}_2\text{O}_3$  is 91 wt.% and 9 wt.% for  $\text{BaCO}_3$  phase. Milling process causes enriching of surface layer of powder particles by  $\text{Fe}_2\text{O}_3$ .

The distribution of powder particles size of mixture  $\text{Fe}_2\text{O}_3$  and  $\text{BaCO}_3$  powders milled for 10, 20, 30 hours is presented in Figure 9. The sizes of tested powders and their statistical means are presented in Table 2.

The arithmetic mean diameter of examined population of  $\text{Fe}_2\text{O}_3$  and  $\text{BaCO}_3$  powders after 10 hours of milling is 4.43(1)  $\mu\text{m}$ . The representative diameter of examined powders (median) has a value of 3.16(5)  $\mu\text{m}$ . After 20 hours of milling the arithmetic

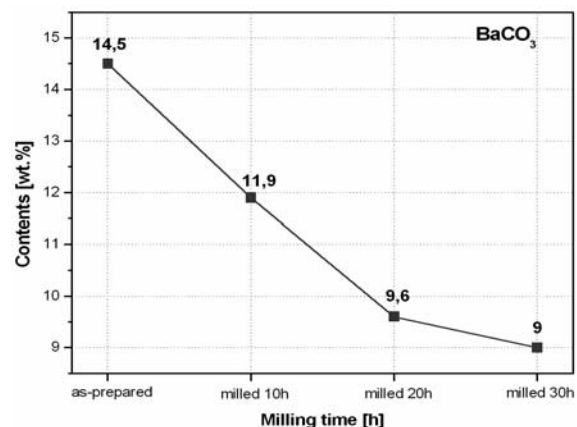


Fig. 8. Contents of  $\text{BaCO}_3$  phase in as-prepared state and after different times of milling

mean diameter has a value of 6.63(8)  $\mu\text{m}$  and median reaches a value of 4.06(5)  $\mu\text{m}$ .

Moreover, the arithmetic mean diameter of tested powders after 30 hours of milling is 7.20(5)  $\mu\text{m}$  and median has a value of 4.82(9)  $\mu\text{m}$ .

Figure 10 shows the morphology of tested mixture  $\text{Fe}_2\text{O}_3$  and  $\text{BaCO}_3$  powders and observed by the scanning electron microscope. From morphology images and distribution of powder particle size can be concluded, that the size of tested powder particles increases with increasing time of milling process.

After 10 hours of milling the shape of tested powder particles is irregular. Figure 10a shows a large quantity of small particles. The increase of milling time up to 20 hours leads to joining of smaller particles in bigger ones, which form agglomerates (Fig.10b). After 30 hours of milling process the quantity of agglomerates increase. The agglomerates are getting to have regular and spherical shape (Fig.10c).

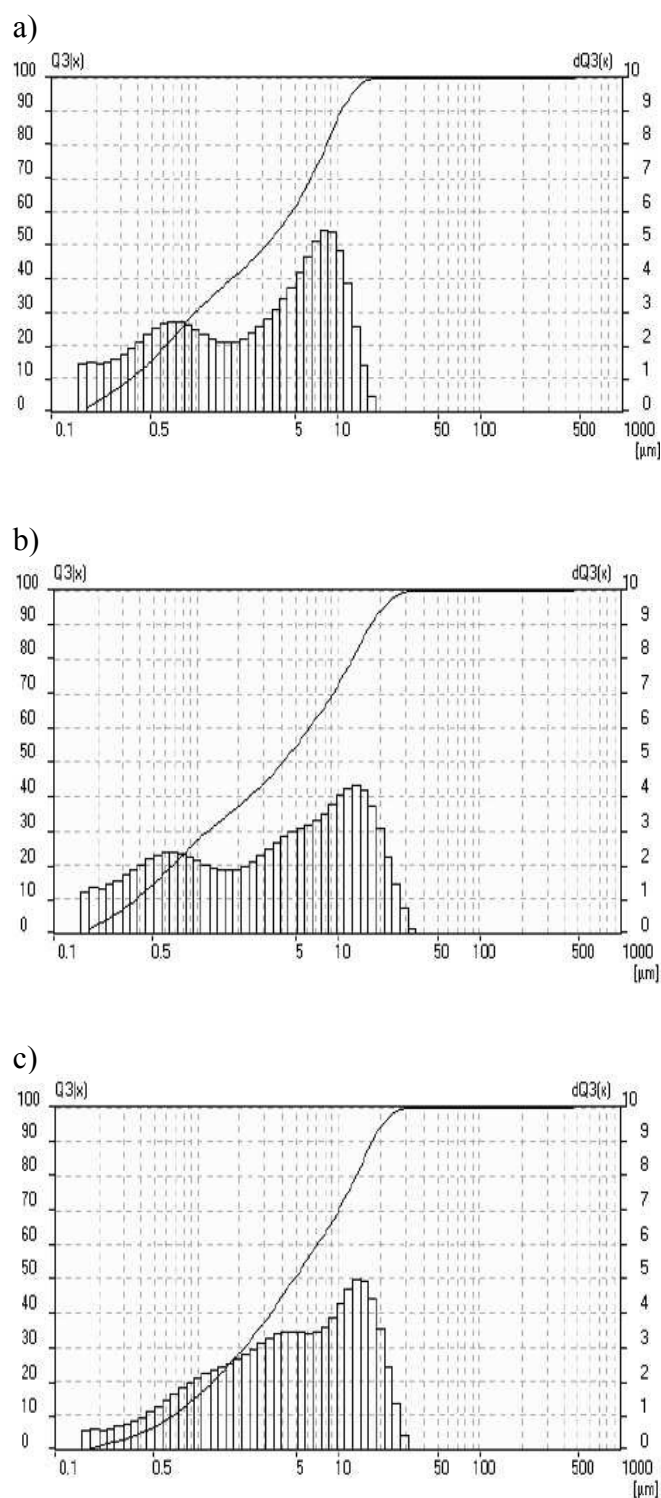


Fig. 9. Distribution and summary curve of powder particle size of  $\text{Fe}_2\text{O}_3$  and  $\text{BaCO}_3$  mixture after different milling times: a) 10 h, b) 20 h, c) 30 h

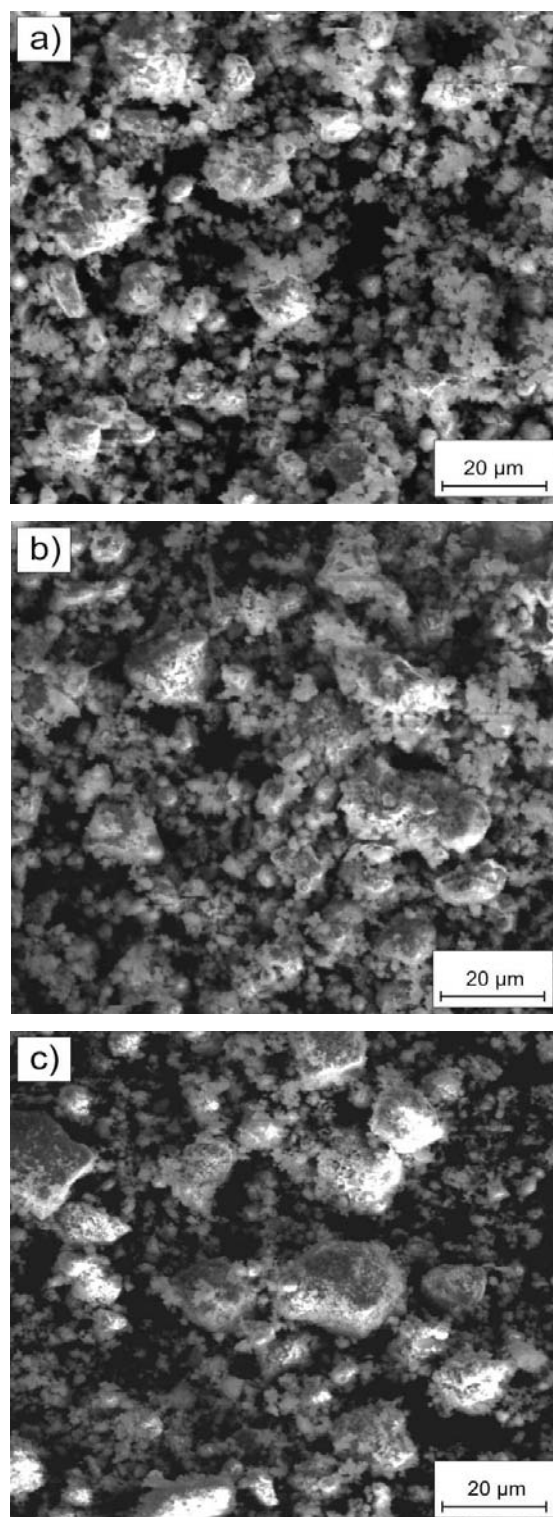


Fig. 10. SEM images of  $\text{Fe}_2\text{O}_3$  and  $\text{BaCO}_3$  mixture after different milling times: a) 10 h, b) 20 h, c) 30 h

Table 2.

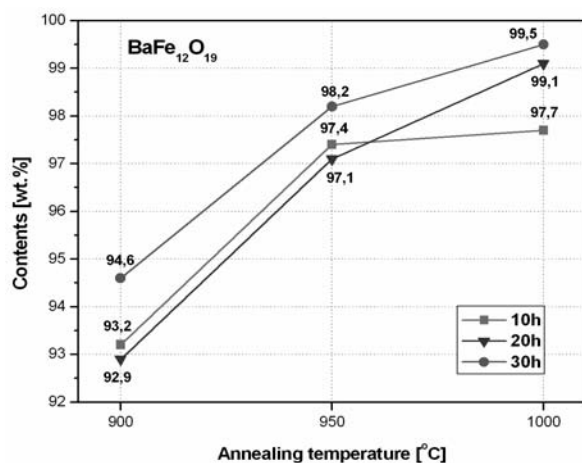
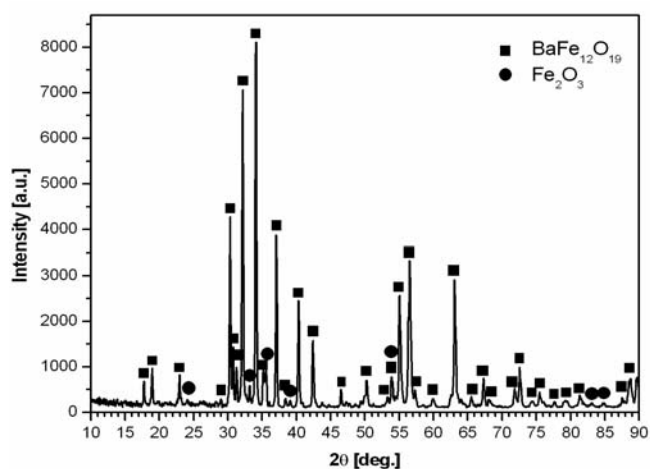
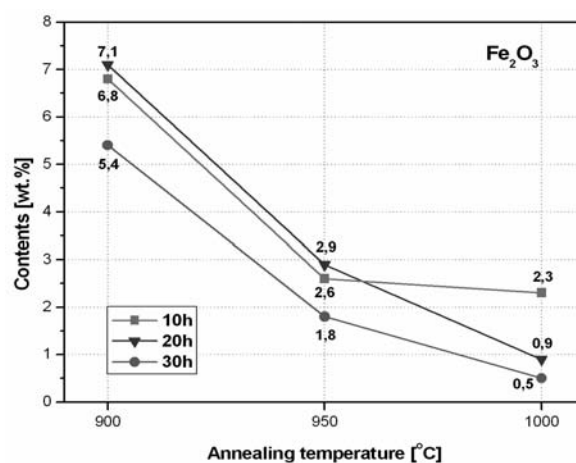
Statistical means and powder particle size of  $\text{Fe}_2\text{O}_3$  and  $\text{BaCO}_3$  mixture after different time of milling process

No.	Powder particle size [ $\mu\text{m}$ ]	Milling time		
		10 h	20h	30h
1.	Arithmetic mean diameter	4.43(1)	6.63(8)	7.20(5)
2.	Geometric mean diameter	2.36(7)	3.07(4)	4.03(8)
3.	Quadratic square mean diameter	6.03(3)	9.56(9)	9.78(8)
4.	Harmonic mean diameter	1.03(3)	1.13(3)	1.74(1)
5.	Standard deviation	2.10(5)	2.57(6)	2.68(4)
6.	Median	3.16(5)	4.06(5)	4.82(9)

The X-ray diffraction investigations of  $\text{Fe}_2\text{O}_3$  and  $\text{BaCO}_3$  mixture milled for 30 hours and annealed at  $950^\circ\text{C}$  enabled the identification of hard magnetic  $\text{BaFe}_{12}\text{O}_{19}$  phase (Fig.11). Moreover, the X-ray analysis also revealed presence of  $\text{Fe}_2\text{O}_3$  phase in examined material. The iron oxide ( $\text{Fe}_2\text{O}_3$ ) is a rest of  $\text{BaCO}_3$  dissociation in the presence of  $\text{Fe}_2\text{O}_3$ , which forms a compound of  $\text{BaFe}_{12}\text{O}_{19}$ . The X-ray diffraction patterns of  $\text{Fe}_2\text{O}_3$  and  $\text{BaCO}_3$  mixture after different times of milling and annealing at  $950^\circ\text{C}$  are presented in Figure 14.

Moreover, the annealing and milling process causes increase content of hard magnetic phase ( $\text{BaFe}_{12}\text{O}_{19}$ ) obtain after heat treatment and decrease of  $\text{Fe}_2\text{O}_3$  phase. The effect of annealing temperature (900, 950,  $1000^\circ\text{C}$ ) on content of  $\text{BaFe}_{12}\text{O}_{19}$  and  $\text{Fe}_2\text{O}_3$  phases for different times of milling is presented in Figure 12 and 13.

After 30 hours of milling process and annealing at  $1000^\circ\text{C}$  content of  $\text{BaFe}_{12}\text{O}_{19}$  phase reaches a value of 99.5 wt.%. the increase of milling time and temperature of annealing leads to increase content of tested hard magnetic phase.

Fig. 12. Contents of  $\text{BaFe}_{12}\text{O}_{19}$  phase after: 10, 20, 30 hours of milling and annealing at 900, 950 and  $1000^\circ\text{C}$ Fig. 11. X-ray diffraction pattern of  $\text{Fe}_2\text{O}_3$  and  $\text{BaCO}_3$  mixture after 30 hours of milling and annealing at  $950^\circ\text{C}$ Fig. 13. Contents of  $\text{Fe}_2\text{O}_3$  phase after: 10, 20, 30 hours of milling and annealing at 900, 950 and  $1000^\circ\text{C}$

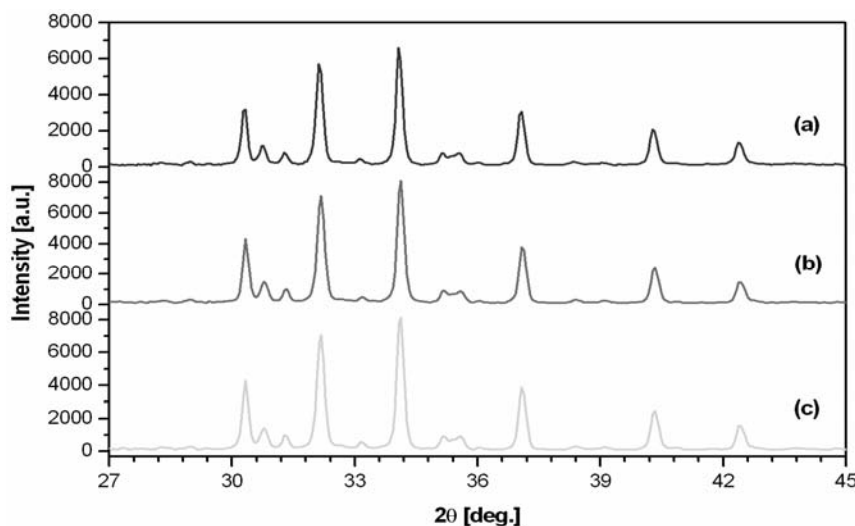


Fig. 14. X-ray diffraction patterns of  $\text{Fe}_2\text{O}_3$  and  $\text{BaCO}_3$  mixture after: a) 10 h, b) 20 h, c) 30 h of milling and annealing at  $950^\circ\text{C}$

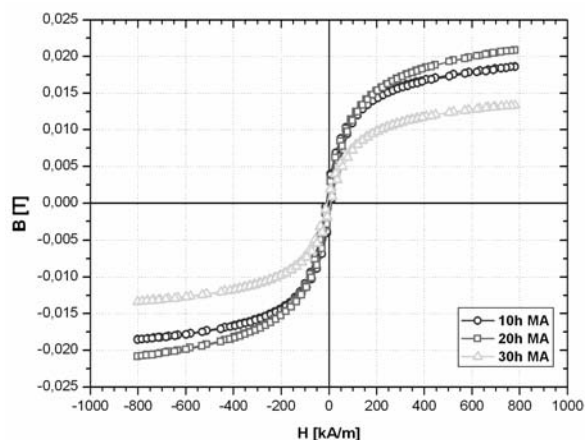


Fig. 15. Hysteresis loops of  $\text{Fe}_2\text{O}_3$  and  $\text{BaCO}_3$  mixture after different milling times

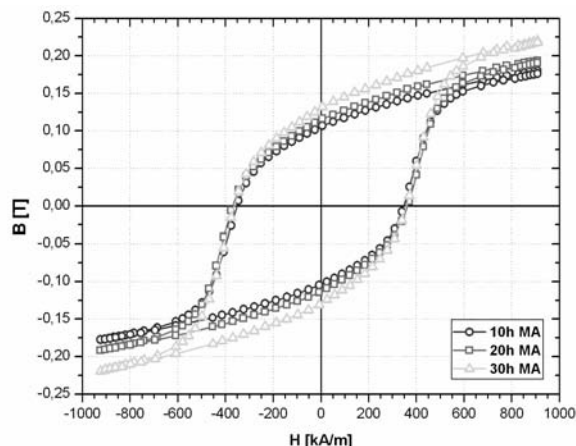


Fig. 16. Hysteresis loops of  $\text{Fe}_2\text{O}_3$  and  $\text{BaCO}_3$  mixture after different milling times and annealing at  $950^\circ\text{C}$

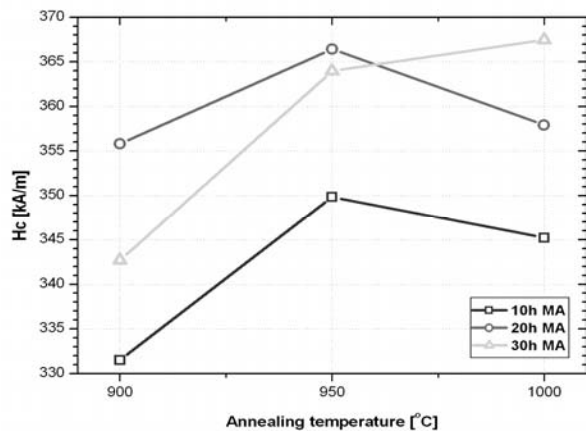


Fig. 17. Coercive force as a function of annealing temperature of  $\text{Fe}_2\text{O}_3$  and  $\text{BaCO}_3$  mixture for different milling times

The hysteresis loops of  $\text{Fe}_2\text{O}_3$  and  $\text{BaCO}_3$  mixture after different times of ball milling is shown in Figure 15. The hard magnetic properties of tested mixture are very low, because of lack of hard magnetic phase. The effect of annealing temperature ( $950^\circ\text{C}$ ) on magnetic properties of  $\text{Fe}_2\text{O}_3$  and  $\text{BaCO}_3$  mixture for different times of milling is presented in Figure 16.

Sample annealed at  $950^\circ\text{C}$  have high value of coercivity. The best coercive force for mixture of powders annealed at  $950^\circ\text{C}$  is 349 kA/m, 366 kA/m and 364 kA/m after 10, 20 and 30 hours of milling, respectively. The high values of coercivity are certainly associated with the microstructure of investigated powder samples.

The coercivity decreases with increasing temperature of annealing above  $950^\circ\text{C}$ , as shown in Figure 17. This effect is related with increasing of the crystallite size at higher temperatures.

## 4. Conclusions

The investigations performed on the  $\text{Fe}_2\text{O}_3$  and  $\text{BaCO}_3$  mixture after milling and heat treatment allowed to formulate the following statements:

- the milling process of  $\text{Fe}_2\text{O}_3$  and  $\text{BaCO}_3$  mixture leads to crystallite refinement and increase the content of  $\text{Fe}_2\text{O}_3$  phase and decrease the of  $\text{BaCO}_3$  content. Milling process causes enriching of surface layer of powder particles by  $\text{Fe}_2\text{O}_3$ ,
- the X-ray diffraction investigations of tested mixture milled for 30 hours and annealed at  $950^\circ\text{C}$  enabled the identification of  $\text{BaFe}_{12}\text{O}_{19}$  and  $\text{Fe}_2\text{O}_3$  phases,
- the annealing and milling process causes increase content of hard magnetic phase ( $\text{BaFe}_{12}\text{O}_{19}$ ) obtain after heat treatment,
- the coercive force of studied powders is dependent on time of ball milling and temperature of their annealing,
- the best coercive force was obtained for powders annealed at temperature of  $950^\circ\text{C}$ ,
- the SEM images and distribution of powder particle size showed that the size of tested powder particles increases with increasing time of milling process,
- the increase of milling time up to 20 hours leads to joining of smaller particles in bigger ones, which form agglomerates.

## Acknowledgements

The authors would like to thank Mr. M. Jodkowski, MSc (Faculty of Chemistry, Silesian University of Technology) for the measuring distribution of  $\text{Fe}_2\text{O}_3$  and  $\text{BaCO}_3$  powder mixture after different time of milling process.

## References

- [1] J. Qiu, M. Gu, Magnetic nanocomposite thin films of  $\text{BaFe}_{12}\text{O}_{19}$  and  $\text{TiO}_2$  prepared by sol-gel method, *Applied Surface Science* 252 (2005) 888-892.
- [2] B. Ziębowicz, D. Szewieczek, L.A. Dobrzański, New possibilities of application of composite materials with soft magnetic properties, *Journal of Achievements in Materials and Manufacturing Engineering* 20 (2007) 207-210.
- [3] L.A. Dobrzański, M. Drak, B. Ziębowicz, Materials with specific magnetic properties, *Journal of Achievements in Materials and Manufacturing Engineering* 17 (2006) 37-40.
- [4] M. Drak, L.A. Dobrzański, Corrosion of Nd-Fe-B permanent magnets, *Journal of Achievements in Materials and Manufacturing Engineering* 20 (2007) 239-241.
- [5] N. Shams, X. Liu, M. Matsumoto, A. Morisako, Manipulation of crystal orientation and microstructure of barium ferrite thin film, *Journal of Magnetism and Magnetic Materials* 290-291 (2005) 138-140.
- [6] O. Carp, R. Barjega, E. Segal, M. Brezeanu, Nonconventional methods for obtaining hexaferrites, *Thermochimica Acta* 318 (1998) 57-62.
- [7] J. Ding, W.F. Miao, P.G. McCormick, R. Street, High-coercivity ferrite magnets prepared by mechanical alloying, *Journal of Alloys and Compounds* 281 (1998) 32-36.
- [8] A. Mali, A. Ataie, Structural characterization of nanocrystalline  $\text{BaFe}_{12}\text{O}_{19}$  powders synthesized by sol-gel combustion route, *Scripta Materialia* 53 (2005) 1065-1075.
- [9] M.H. Makled, T. Matsui, H. Tsuda, H. Mabuchi, M.K. El-Mansy, Magnetic and dynamic mechanical properties of barium ferrite-natural rubber composites, *Journal of Materials Processing Technology* 160 (2005) 229-233.
- [10] W. Martienssen, H. Warlimont, *Springer Handbook of Condensed Matter and Materials Data*, Springer, 2005.
- [11] J. Konieczny, L.A. Dobrzański, A. Przybył, J.J. Wysocki, Structure and magnetic properties of powder soft magnetic materials, *Journal of Achievements in Materials and Manufacturing Engineering* 20 (2007) 139-142.
- [12] P. Gramatyka P., A. Kolano-Burian, R. Kolano, M. Polak, Nanocrystalline iron based powder cores for high frequency applications, *Journal of Achievements in Materials and Manufacturing Engineering* 18 (2006) 99-102.
- [13] The Rietveld method, Edited by R.W. Young, *IUCr Monograph on Crystallography Vol. 5*, Oxford Science Publisher, 1993.
- [14] G. Dercz, K. Prusik, L. Pająk, Structure investigations of commercial zirconia ceramic powder, *Journal of Achievements in Materials and Manufacturing Engineering* 18 (2006) 259-262.
- [15] R. Nowosielski, R. Babilas, G. Dercz, L. Pająk, Microstructure of composite material with powders of barium ferrite, *Journal of Achievements in Materials and Manufacturing Engineering* 17 (2006) 117-120.
- [16] R. Nowosielski, R. Babilas, G. Dercz, L. Pająk, J. Wrona, Barium ferrite powders prepared by milling and annealing, *Journal of Achievements in Materials and Manufacturing Engineering* 22/1 (2007) 45-48.
- [17] J. Wrona, T. Stobiecki, M. Czapkiewicz, R. Rak, T. Ślęzak, J. Korecki and C. G. Kim, R-VSM and MOKE magnetometers for nanostructures, *Journal of Magnetism and Magnetic Materials* 272-276/P3 (2004) 2294-2295.